Progress In Electromagnetics Research C, Vol. 97, 57–67, 2019

A Planar Wideband Two-Level Sequentially Rotated Array Antenna for X-Band CubeSat

Son Xuat Ta*, Khac Kiem Nguyen, and Chien Dao-Ngoc

Abstract—A planar wideband circularly-polarized (CP) antenna array is designed for an X-band CubeSat. The design is a two-level sequential phase architecture, consisting of a 4×4 element array composed of sequentially rotated of 2×2 subarrays. Each subarray consists of sequentially rotated 2×2 antennas using metasurface. These antenna elements are incorporated with a two-level sequentially rotated phase network in order to obtain wideband characteristic and high gain. The final prototype with a size of 100 mm × 100 mm × 2.032 mm yields a measured $|S_{11}| < -10$ dB bandwidth of 50% (6–10 GHz) and measured axial ratio < 3-dB bandwidth of 40.7% (6.45–9.75 GHz). Additionally, the proposed design achieves a good broadside right-hand CP radiation with a peak gain of 17.0 dBic, 3-dB gain bandwidth of 20.4% (7.5–9.2 GHz), and radiation efficiency of > 82%. With these features, the proposed antenna can be compatible with any CubeSat standard structure, as well as other small satellites.

1. INTRODUCTION

CubeSat, which is a kind of pico-satellite, has become a hot topic of research owing to its short-time development, low cost, and potential to provide multifunction capabilities [1]. A CubeSat is made up of multiples of cubic units; each unit has a side dimension of 10 cm and a mass of no more than 1-kg [2]. In the early CubeSats, deployable wire antennas operating at VHF/UHF bands are typically used for the low bitrate links (tele-command and telemetry), while S-band antennas are typically used for the high bitrate links of payload data [3]. Along with the demand of broader bandwidth for downloading more data at higher bitrate, recently, X-band frequencies are used for transmitting the payload data of CubeSats [4]. Accordingly, high-gain X-band CubeSat antennas have received much attention. With the main feature of high gain, reflector antennas [5, 6] and reflectarray antennas [7] have been popular choices for CubeSat high-speed data downloading. The sizes of these antennas are normally much larger than the CubeSat bodies, and therefore, the methods to stow the antennas are required. Inflatable and deployable methods [5–7] enable stowing an antenna inside a small volume and fully deploying in orbit. However, these methods are usually accompanied by increases in the structure complexity and the realization cost of the satellites. As planar antennas [8] with several features — including compact size, light weight, and planar configuration — can be easily integrated on the satellite body, they have been attractive for small satellites. Several developments of the planar array antennas have been proposed for the X-band CubeSat applications. In [9], an X-band 4-patch array antenna was designed to operate at 8080 MHz with a voltage standing wave ratio < 2 bandwidth of 8050–8200 MHz and a gain of 9 dB. An X-band circularly polarized (CP) array was modeled on a 1U CubeSat [10]. The array composed of 2×2 shorted annular patches and a sequential-phase feeding network achieved an axial ratio (AR) < 3 dB at 7.5–8.75 GHz and the peak gain of 13 dBic. With the medium gain (up to $\sim$ 13 dBic), these 4-patches array antennas are suitable for CubeSat satellites without high-precision

Received 28 September 2019, Accepted 19 November 2019, Scheduled 26 November 2019
* Corresponding author: Son Xuat Ta (xuat.tason@hust.edu.vn).
The authors are with the School of Electronics and Telecommunications, Hanoi University of Science and Technology, Ha Noi, Viet Nam.

attitude determination and control system. In order to further increase the gain and broaden the AR bandwidth, planar array antennas have been incorporated with two-level sequentially rotated feeding networks [11–14]. Typically, the feeding networks [11, 12] utilized microstrip lines with different electric lengths to achieve the desired phases, and consequently, they required a large area for deploying the microstrip lines. The compact array antennas [13, 14] used series-parallel strips with curved structures in their feeding networks. These arrays employed narrow-band primary radiation elements, i.e., slotted disk-based patch [13] or truncated-corner patch [14], and therefore, their operational bandwidths were only up to 14% or less.

In this paper, a planar, high-gain, wideband, CP antenna with simple configuration and low realization cost is presented for X-band CubeSat applications. The antenna is composed of 4×4 antennas using metasurface [15] which are incorporated with a two-level sequential phase network to not only achieve the high-gain and the wideband operation, but also be compatible with any CubeSat standard structure. The antenna is designed on two low-cost substrates (Subs. #1 and #2) of Rogers RO4003 sheet; i.e., the patch array and the feeding network are built on the top side of Sub. #1, while the metasurfaces are built on the top side of Sub. #2. For easy realization and small height, the two substrates are stacked together without an air gap. The advantages of the design are demonstrated by using the ANSYS Electronic Desktop and validated experimentally.

2. ANTENNA DESIGN

2.1. Configuration of Two-Level Sequentially Rotated CP Array

Sequential rotation technique [16] has been presented as a common way to generate a CP radiation with linearly polarized patch antennas or to improve the radiation performances of CP patch antennas.

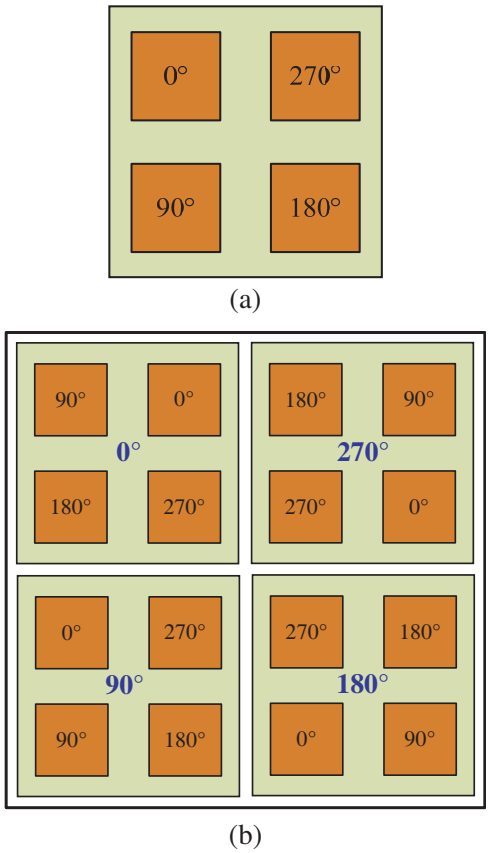

Figure 1. Basic design of (a) one-level and (b) two-level sequentially rotated patch array.

Fig. 1(a) shows the basic configuration of a conventional sequentially rotated patch array. As shown, four radiating elements are sequentially rotated and fed by four ports with the same magnitude and phases of 0°, 90°, 180°, and 270°, respectively. In order to further improve the bandwidth, as well as polarization purity, a two-level sequentially rotated patch array is implemented. As shown in Fig. 1(b), this design consists of 2×2 one-level sequentially rotated arrays, named as subarrays, which are arranged in a rotation sequence. Fig. 1 serves as a guide for designing and optimizing the proposed structure using metasurface-based antennas [15], which is demonstrated in the following sections.

2.2. Antenna Geometry

Figure 2 shows the geometry of the proposed antenna array, which is a planar structure with footprint of 100 mm × 100 mm to be compatible with any CubeSat standard structure. It consists of 4×4 metasurface-based antennas, which are formed in a two-level sequentially rotated array and fed by a feeding network composed of 5 sequentially rotated phase networks based on series-parallel strips [17]. The antenna system is built on two Rogers RO4003 substrates (Sub. #1 and Sub. #2) with permittivity of 3.38, loss-tangent of 0.0027, and thicknesses of $h_1 = 0.508$ mm (20 mil) and $h_2 = 1.524$ mm (60 mil), nevertheless keeping a planar configuration with a total thickness of 2.032-mm (80 mil). The patches and two-level sequential phase network are built on the top side of Sub. #1. The metasurfaces are built on the top side of Sub. #2. The input of the feeding network is a 50-Ω sub-minimization version-A (SMA) connector. For easy realization, the two substrates are stacked together without an air gap.

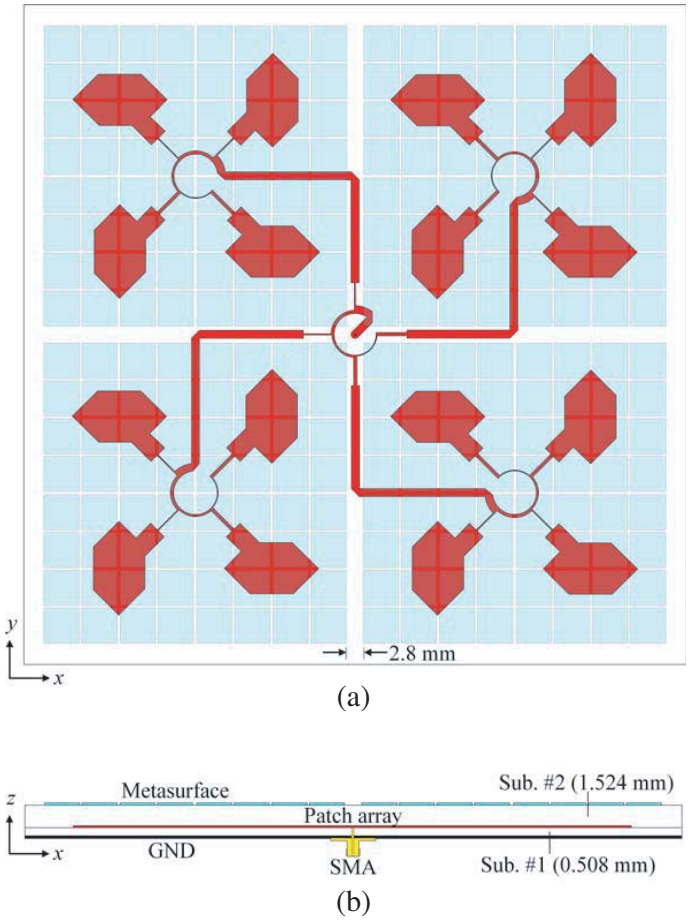

Figure 2. Geometry of the proposed array antenna: (a) top-view and (b) side-view.

2.3. Sequentially Rotated Phase Network

Figure 3(a) illustrates the geometry of the sequentially rotated phase network. The network is a series-parallel strip with a curved structure [17], which is compensated for the Rogers RO4003 substrates and optimized for equally distributing the signal from the input to four outputs with progression phases of 90°. The input and outputs are microstrip-lines with $\sim$ 50-Ω characteristic impedance. The input is directly connected to the SMA connector. In order to achieve sequential phases and impedance matching, the network uses seven quarter-wavelength impedance transformers, which are linked together in a sequential rotation manner with alternative parallel and series connections. The network is designed for the center frequency of 8.2 GHz, and its optimized parameters are as follows: $W_{ms} = 1.1$, $L_a = 5.0$, $R_i = 3.2$, $w_1 = 0.2$, $w_2 = 0.7$, $w_3 = 0.2$, $w_4 = 0.5$, $w_5 = 0.5$, $w_6 = 0.2$, and $w_7 = 0.5$ (Units: mm). The sequentially rotated phase network is characterized via the ANSYS Electronic Desktop, and its S-parameters and output phases are given in Figs. 3(b) and (c), respectively. It is observed that the reflection coefficient $|S_{11}|$ of the network is less than −15 dB at 6–10 GHz, and the transmission coefficients of the four outputs are almost equal at 7–9 GHz. From Fig. 3(c), the output phases of the network achieves the expected 90° progression within the interest frequency range.

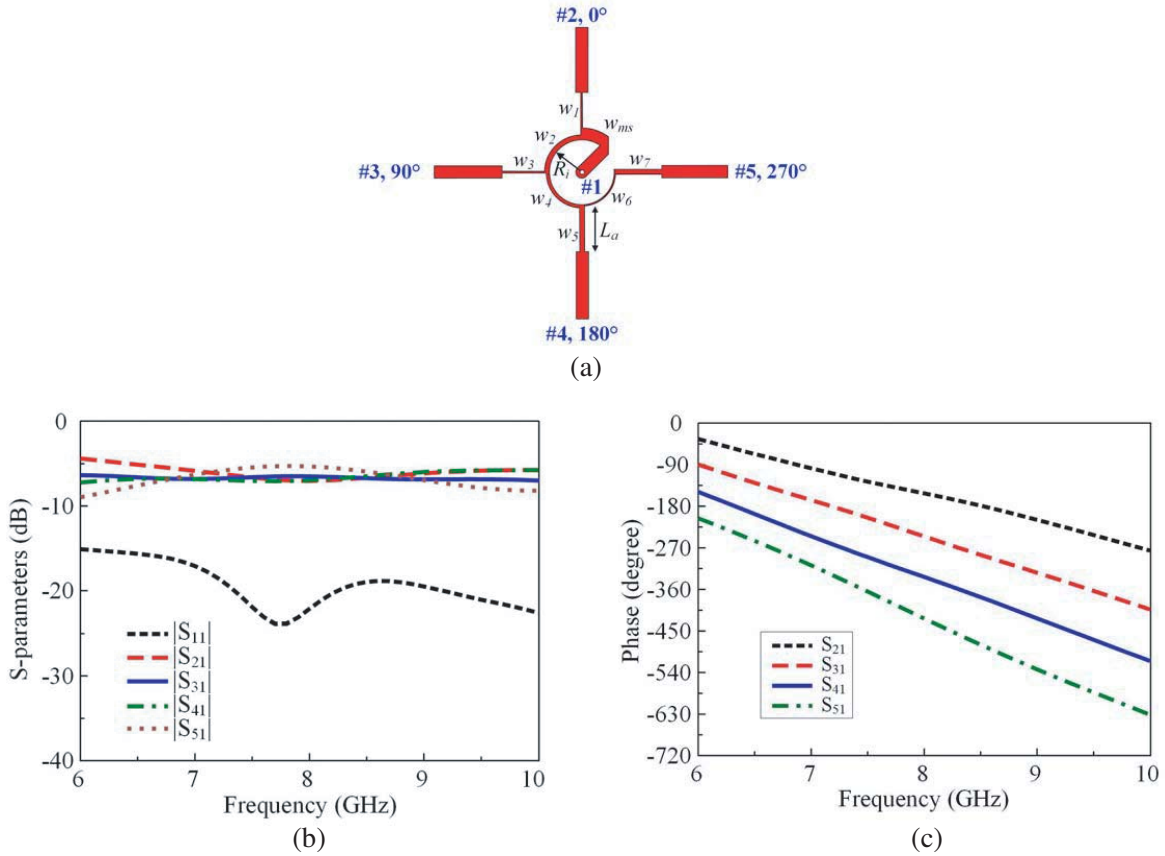

Figure 3. Sequentially rotated phase network: (a) geometry, (b) S-parameters, and (c) phases.

2.4. Subarray

The geometry of the subarray is illustrated in Fig. 4. The subarray consists of 2 × 2 patch antennas using metasurface and is fed by a sequentially rotated phase network. Different from [15], the driven patch of the antenna element is rotated 45° in order to easily deploy the entire array (4 × 4 elements) on the given area of 100 mm × 100 mm. The feeding network of the subarray is same as the optimized one presented in the previous section. The subarray design is optimized to obtain a wideband characteristic

and high gain at the center frequency of 8.2 GHz. Referring to Fig. 4, the optimized design parameters of the subarray are as follows: $P = 5.7$, $g = 0.4$, $gap = 0.6$, $W_{ms} = 1.1$, $L_a = 5.0$, $R_i = 3.2$, $w_1 = 0.2$, $w_2 = 0.7$, $w_3 = 0.2$, $w_4 = 0.5$, $w_5 = 0.5$, $w_6 = 0.2$, $w_7 = 0.5$, $W_p = 10$, $L_c = 4.5$, $W_s = 3.0$, $L_s = 3.2$, and $S_p = 23$ (Units: mm).

In order to illustrate the effects of the metasurface, different configurations of the 2×2 patch array antenna, as shown in Fig. 5, are investigated. Ant. 1 is a subarray without metasurface. Ant. 2 is a 2×2 patch array, which is fully optimized for broadband CP radiation at the center frequency of 8.2 GHz. Ant. 3 is the subarray of the proposed antenna. The design parameters of Ant. 1 and Ant. 3 are same

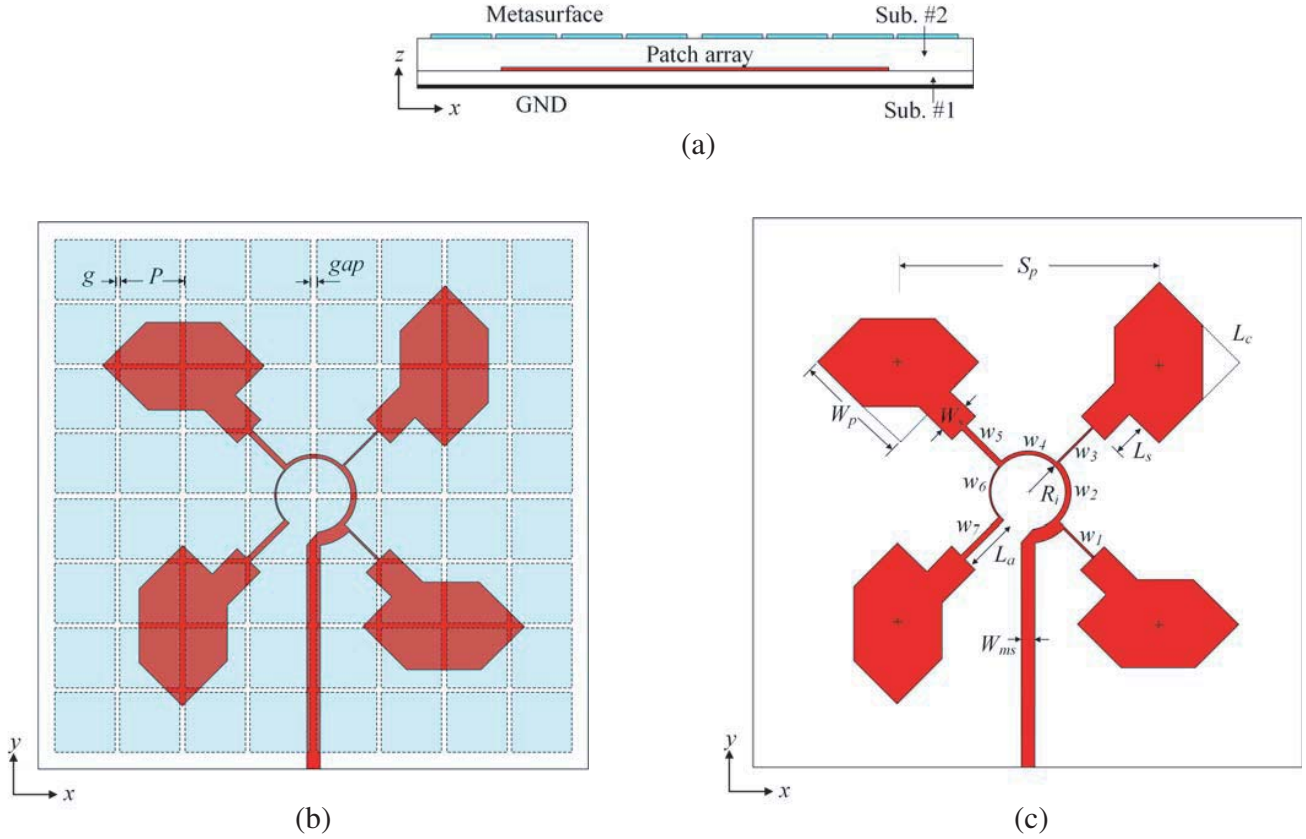

Figure 4. Geometry of the subarray: (a) side-view, (b) top view including metasurface, and (c) top view of the patch antenna array.

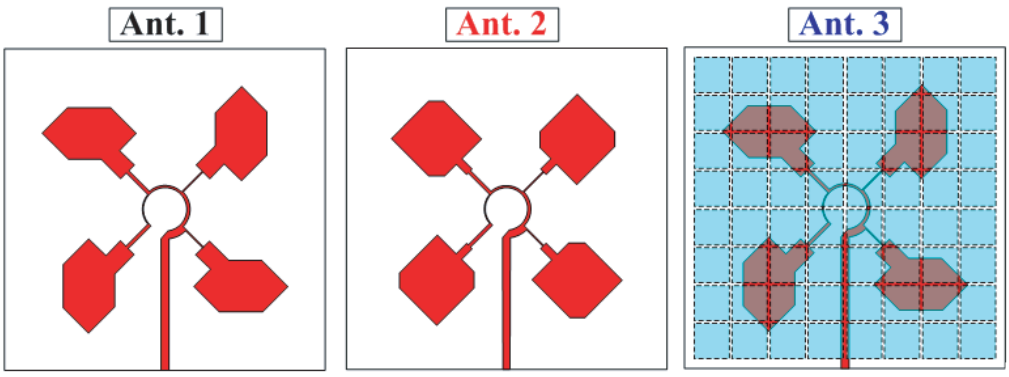

Figure 5. Different configurations of the 2×2 patch array antenna.

as those of the subarray in Fig. 4. Referring to Fig. 3(c), the design parameters of Ant. 2 are as follows: $W_{ms} = 1.1$, $L_a = 5.0$, $R_i = 3.2$, $w_1 = 0.2$, $w_2 = 0.7$, $w_3 = 0.2$, $w_4 = 0.5$, $w_5 = 0.5$, $w_6 = 0.2$, $w_7 = 0.5$, $W_p = 10$, $L_c = 1.5$, $W_s = 0.6$, $L_s = 3.2$, and $S_p = 23$ (Units: mm).

The performances for different configurations of the 2×2 patch array antenna are calculated via the ANSYS Electronic Desktop and given in Fig. 6. It is observed that the presence of the metasurface enhances the antenna performances significantly. As shown in Fig. 6, Ant. 1 yields a poor performance due to the absence of metasurface, and it has not been fully optimized. Both Ant. 2 and Ant. 3 are fully optimized for broadband CP radiation at the center frequency of 8.2 GHz. The patch array without metasurface (Ant. 2) achieves an $|S_{11}| < -10$ dB bandwidth of 10.38% (7.67–8.51 GHz), AR < 3 dB bandwidth of 8.1% (7.69 – 8.34 GHz), and the peak gain of 11.2 dBic. Ant. 3 achieves an $|S_{11}| < -10$ dB bandwidth of 38.1% (6.8–10.0 GHz), AR < 3 dB bandwidth of 27.85% (6.8–9.0 GHz), and the peak gain of 13.16 dBic. Compared to the traditional patch array (Ant. 2), the metasurface-based patch array (Ant. 3) achieves a $\sim$ 360% increase in $|S_{11}| < -10$ dB bandwidth, $\sim$ 340% increase in AR $<$ 3-dB bandwidth, and ~ 2 dB increase in the gain.

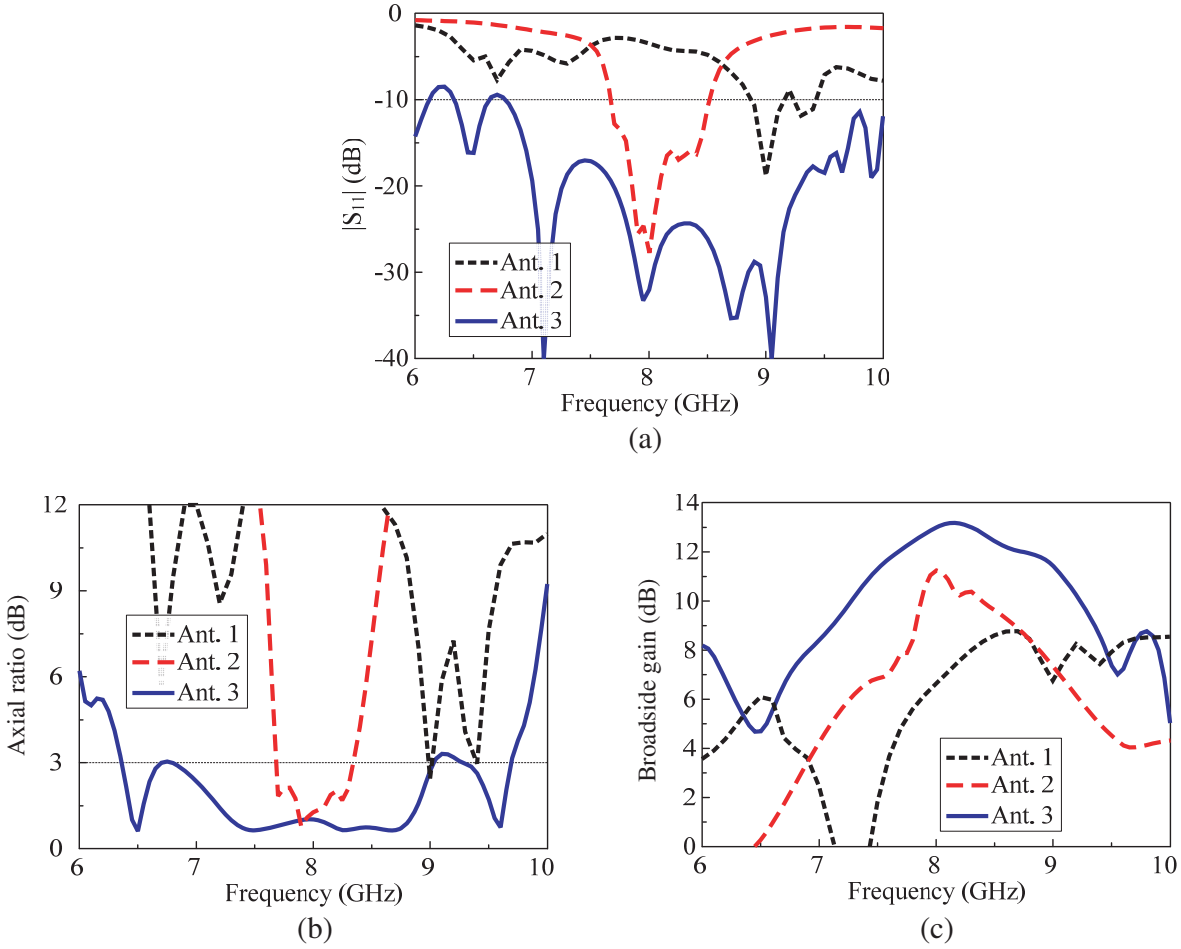

Figure 6. Simulated performances for the different configurations of the 2×2 patch array antenna: (a) $|S_{11}|$, (b) AR, and (c) gain values.

It is well known that the element spacing is a crucial parameter for determining the performances of the sequentially rotated array. In the proposed design, the element spacing is optimized for the maximum broadside gain at 8.2 GHz. This is illustrated in Fig. 7, which shows the performances of the subarray for different element spacings. Note that the metasurface size of the single element is $4 \times P = 22.8$ mm. To avoid overlap, S_p cannot be less than 22.8 mm. As shown in Fig. 7, with the spacing increased, $|S_{11}|$ and |AR| values are hardly changed at the desired frequency range, while the

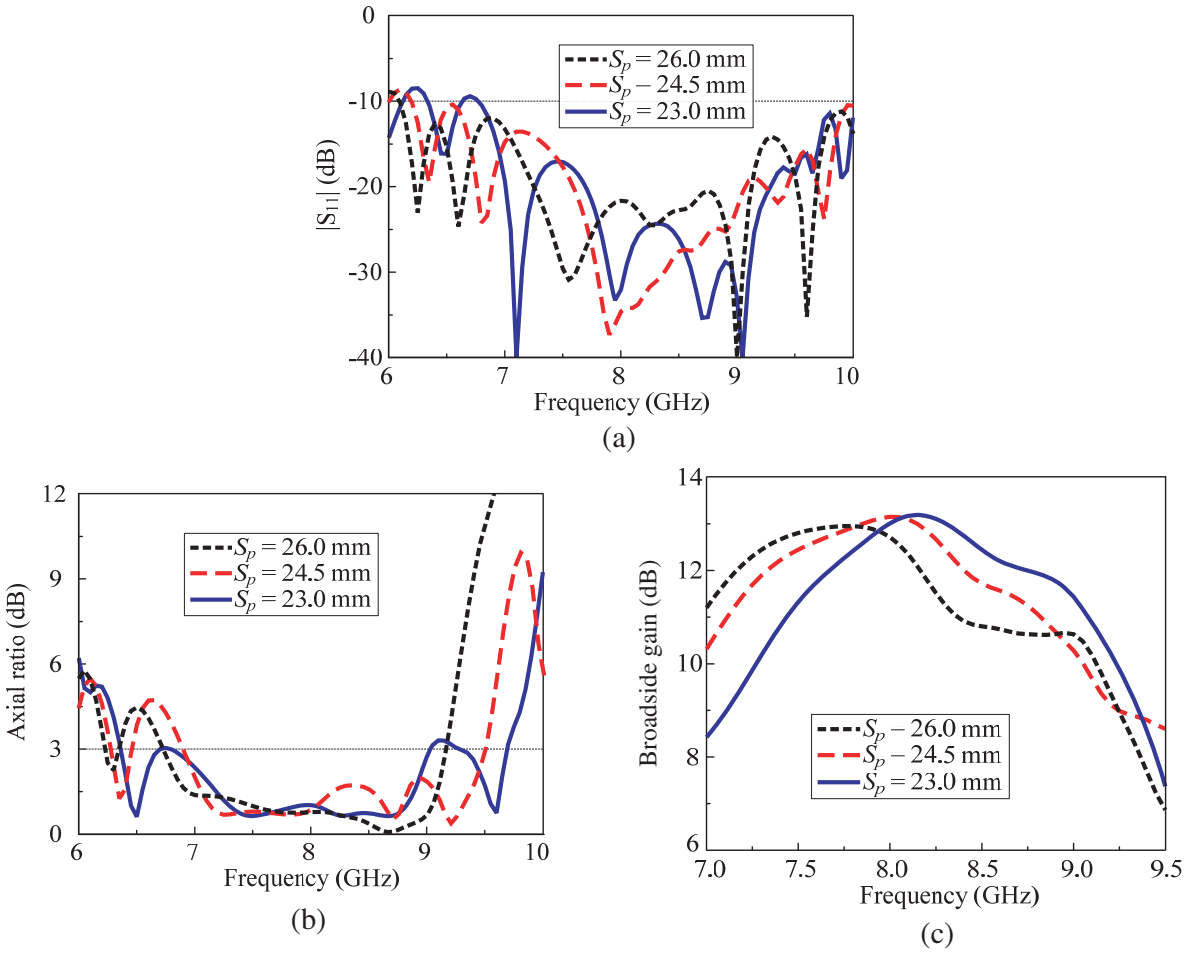

Figure 7. Simulated performances of the subarray for different element spacing: (a) $|S_{11}|$, (b) AR, and (c) broadside gain.

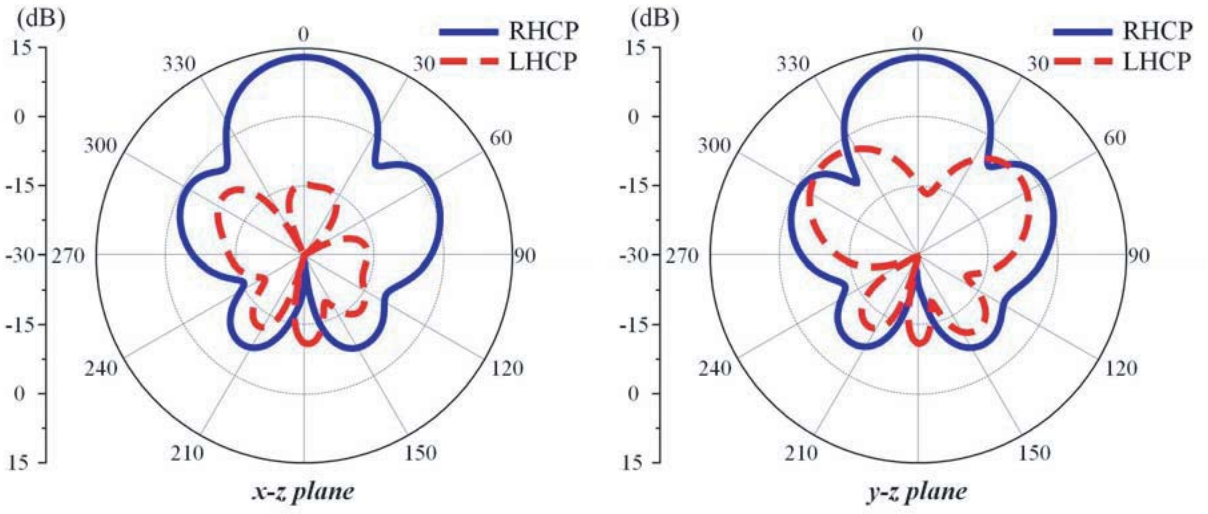

Figure 8. Simulation 8.2-GHz radiation pattern of the subarray.

peak gain shifts toward the lower frequency. $S_p = 23.0$ mm offers the peak gain of 13.16 dBic at the desired frequency of 8.2 GHz, whereas the other cases with $S_p = 24.5$ mm and $S_p = 26.0$ mm yield peak gains at 8.0 GHz and 7.8 GHz, respectively. Accordingly, the $S_p = 23.0$ mm is chosen for the final design.

Figure 8 shows the simulated radiation pattern of the subarray. As expected, the subarray antenna yields a right-hand CP (RHCP) radiation with symmetric profile and high front-to-back (F-B) ratio. At 8.2 GHz, the subarray achieves a gain of 13.16 dBic, an F-B ratio of 28 dB, and half-power beamwidths (HPBW) of 33° in both x-z and y-z planes.

3. FABRICATION AND MEASUREMENTS

The proposed array antenna is fabricated and measured. A fabricated sample of the prototype is given in Fig. 9(a). The patch array with feeding network and metasurface are realized on Rogers RO4003 substrates with a copper thickness of 17 μm via a standard printed circuit board technology. In order to simplify the fabrication, the two substrates are fastened together using thin strips of tape (not included in the simulations). The measured and simulated $|S_{11}|$ and AR values of the prototype are given in Figs. 9(b) and (c). Both simulation and measurement indicate that the design achieves a wideband operation. From Fig. 9(b), the measured $|S_{11}| < -10$ dB bandwidth is 6.0–10.0 GHz (50%), whereas the simulated bandwidth is 6.3–10.0 GHz (45.4%). From Fig. 9(c), the measurements result in a 3-dB AR bandwidth of 6.45–9.75 GHz (40.7%) as compared to the simulation value of 6.35–9.65 GHz (41.25%). A slight discrepancy between the simulation and measurement results could be attributed to the fabrication tolerance; namely, some undesired airs between the two substrates cannot be eliminated.

Figure 10(a) shows the normalized 8.2 GHz radiation pattern of the fabricated prototype. It is observed that the antenna radiates an RHCP wave with symmetric pattern and a high F-B ratio. At 8.2 GHz, the measurements result in an F-B ratio of > 20 dB and HPBWs of 21° and 20° in the x-z and y-z planes, respectively. The broadside gain of the array is given Fig. 10(b). The measurements

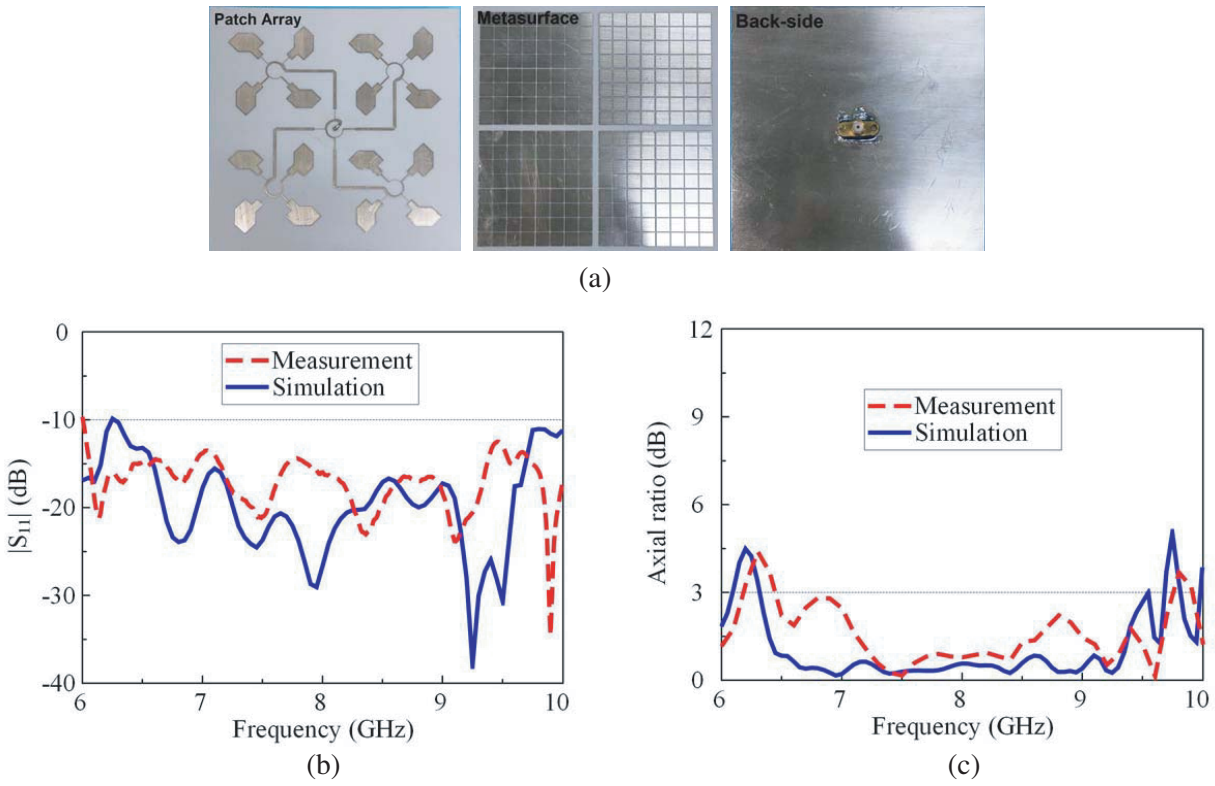

Figure 9. (a) Fabricated sample of the proposed array, (b) $|S_{11}|$, and (c) AR values.

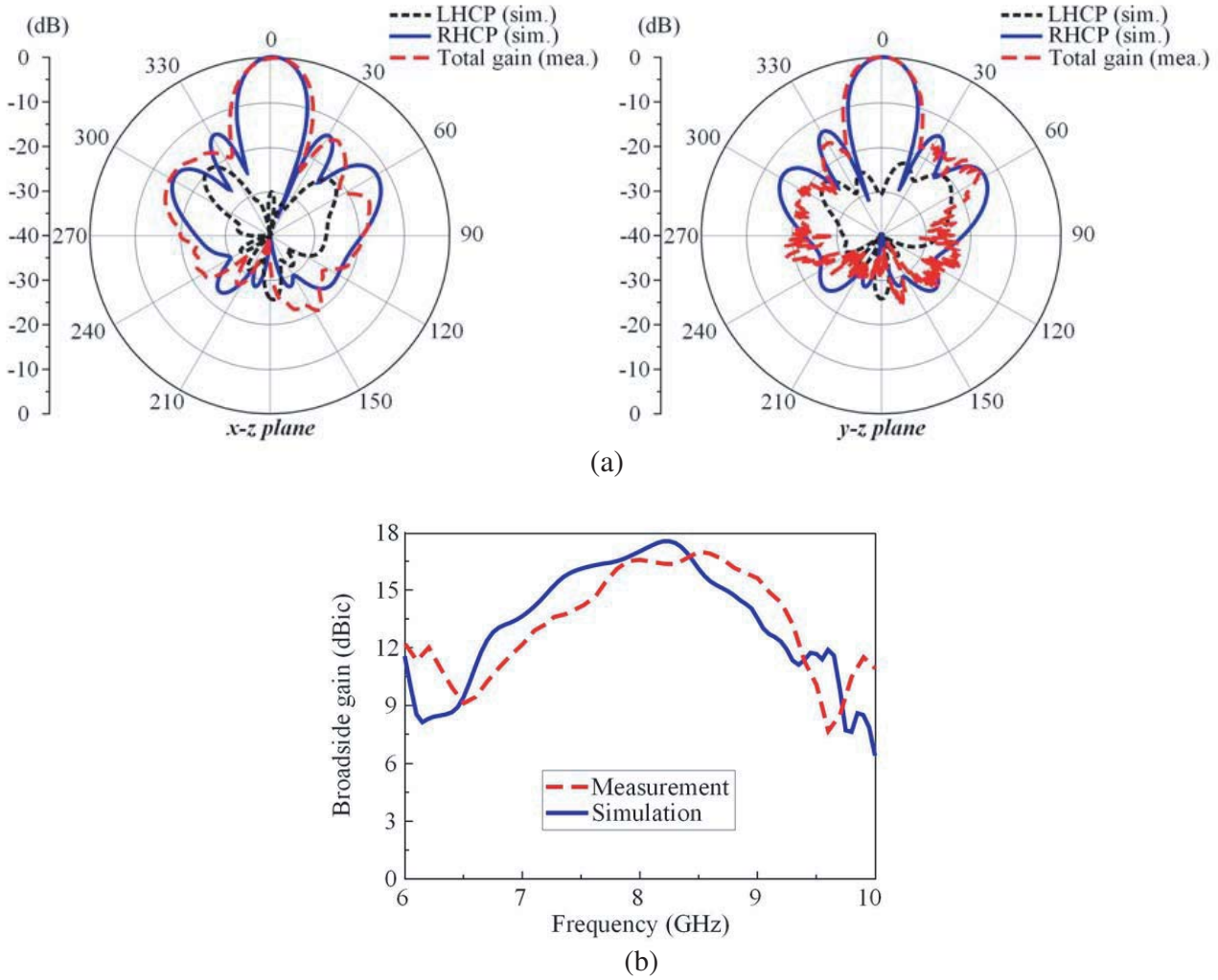

Figure 10. (a) Normalized 8.2 GHz radiation pattern and (b) broadside gain of the proposed array.

result in a 3-dB gain bandwidth of 7.5–9.2 GHz (20.36%) with the peak gain of 17.0 dBic at 8.5 GHz, whereas the simulated 3-dB gain bandwidth is 7.2–8.8 GHz (20%) with the peak gain of 17.6 dBic at 8.25 GHz. Moreover, the measurements result in a high radiation efficiency of $> 82\%$ as compared to the simulated value of $> 85\%$ across the operational bandwidth.

A performance comparison between the proposed array antenna and recent X-band 4×4 element array antennas is given in Table 1. Due to employing dual-feed CP patches as the primary radiating elements [11, 12], these arrays suffer from complex feeding networks; i.e., the dual-feed is realized by a Wilkinson power-divider combined with a 90° phase shifter [11] or a branch-line coupler [12]. Also, the patches and feeding networks are built on different substrates; they are connected by using vias passed through multi-layers. By using series-parallel strips with curved structures, the feeding networks and patches of the proposed array and the priors in [13, 14] are implemented on the top side of a single-layer substrate. As shown in Table 1, our design yields a significantly smaller size, a simpler configuration, and a comparable global bandwidth (the global bandwidth is overlapped bandwidths for $|S_{11}| < -10$ dB, CP radiation, and 3-dB gain) relative to the arrays in [11, 12]. In comparison with the array using single-feed CP elements [13, 14], the proposed antenna achieves a significantly wider global bandwidth, nevertheless a similar complexity.

Table 1. Performance comparison of the proposed design and the recent X-band 4×4 element array antennas.

Antenna structures	Size (λ^3)	Feeding network	Center frequency	$\lvert S_{11}\rvert < -10$ dB BW	CP radiation BW	3-dB gain BW	Gain (dBic)
Proposed	$2.67 \times 2.67 \times 0.054$	simple	8.2 GHz	50.0%	40.7% (AR < 3-dB)	20.4%	17.0
Ref. [11]	$3.47 \times 3.47 \times 0.076$	complex	6.5 GHz	74.8%	47.8% (AR < 1-dB)	14.2%	18.0
Ref. [12]	$3.50 \times 3.50 \times 0.162$	complex	8.0 GHz	25.0%	25.0% (AR < 1-dB)	20.5%	18.2
Ref. [13]	$1.73 \times 1.73 \times 0.035$	simple	6.5 GHz	56%	30.2% (AR < 4-dB)	14%	12.6
Ref. [14]	$2.80 \times 2.80 \times 0.047$	simple	8.0 GHz	12.7%	8.8% (AR < 3-dB)	Not mentioned	16.9

λ is a free space wavelength referring to the center frequency

4. CONCLUSION

A planar antenna array with wideband and high-gain CP radiation has been proposed for X-band CubeSat applications. The array is composed of 4×4 antennas using metasurface, which are formed in a two-level sequentially rotated array and incorporated with a two-level sequentially rotated phase network. The prototype with an overall size of $100\,\text{mm} \times 100\,\text{mm} \times 2.032\,\text{mm}$ achieves an $|S_{11}| < -10$ dB bandwidth of 50%, a 3-dB AR bandwidth of 40.7%, a 3-dB gain bandwidth of 20.36%, the peak gain of 17.0 dBic, and a radiation efficiency of >82%. With these advantages — including simple configuration, planar structure, wide operating frequency band, stable radiation profile, high gain, and high radiation efficiency — the proposed design is a good candidate for use in X-band CubeSat applications, as well as other small satellites.

ACKNOWLEDGMENT

The paper describes a result of the project (VT-CN.03/18-20) funded by the National Program on Space Science and Technology, Vietnam Academy of Science and Technology (VAST).

REFERENCES

1. Gao, S., K. Clark, M. Unwin, J. Zackrisson, W. A. Shiroma, J. M. Akagi, K. Maynard, P. Garner, L. Boccia, G. Amendola, G. Massa, C. Underwood, M. Brenchley, M. Pointer, and M. N. Sweeting, "Antennas for modern small satellites," *IEEE Antennas Propag. Mag.*, Vol. 51, No. 4, 40–56, 2009.
2. Rodriguez-Osorio, R. M. and E. F. Ramirez, "A hands-on education project: Antenna design for inter-CubeSat communications," *IEEE Antennas Propag. Mag.*, Vol. 54, No. 5, 211–224, Oct. 2012.
3. Rahmat-Samii, Y., V. Manohar, and J. M. Kovitz, "For satellites, think small, dream big," *IEEE Antennas Propag. Mag.*, Vol. 59, No. 2, 22–30, Apr. 2017.
4. Gao, S., Y. Rahmat-Samii, R. E. Hodges, and X. Yang, "Advanced antennas for small satellites," *IEEE Proc.*, Vol. 106, No. 3, 391–403, Mar. 2018.
5. Babuscia, A., T. Choi, J. Sauder, A. Chandra, and J. Thangavelautham, "Inflatable antenna for CubeSats: Development of the X-band prototype," *Proc. IEEE Aerosp. Conf.*, 1–11, Big Sky, MT, USA, Mar. 2016.
6. Babuscia, A., J. Sauder, A. Chandra, J. Thangavelautham, L. Feruglio, and N. Bienert, "Inflatable antenna for CubeSat: A new spherical design for increased X-band gain," *Proc. IEEE Aerosp. Conf.*, 1–10, Big Sky, MT, USA, Mar. 2017.

7. Hodges, R. E., N. Chahat, D. J. Hoppe, and J. D. Vacchione, "A deployable high-gain antenna bound for Mars: Developing a new folded-panel reflectarray for the first CubeSat mission to Mars," *IEEE Antennas Propag. Mag.*, Vol. 59, No. 2, 39–49, Apr. 2017.
8. Tubbal, F., R. Raad, and K. Chin, "A survey and study of planar antennas for pico-satellites," *IEEE Access*, Vol. 3, 2590–2612, 2015.
9. Altunc, S., O. Kegege, S. Bundick, H. Shaw, S. Shaire, G. Bussey, G. Crum, J. C. Burke, S. Palo, and D. O'Conor, "X-band CubeSat communication system demonstration," *29th Annual AIAA/USU Conference Small Satellite*, Logant, UT, USA, Aug. 2015.
10. Lehmensiek, R., "Design of a wideband circularly polarized 2×2 array with shorted annular patches at X-band on a CubeSat," *2017 International Symposium on Antennas and Propagation*, Phuket, Thailand, 2017.
11. Hu, Y., W. Ding, and W. Cao, "Broadband circularly polarized microstrip antenna array using sequentially rotated technique," *IEEE Antennas Wireless Propag. Lett.*, Vol. 10, 1358–1361, 2011.
12. Garcia-Aguilar, A., J. M. Inclan-Alonso, L. Vigil-Herrero, J. M. Fernandez-Gonzalez, and M. Sierra-Perez, "Low-profile dual circularly polarized antenna array for satellite communications in the X band," *IEEE Trans. Antennas Propag.*, Vol. 60, No. 5, 2276–2284, May 2012.
13. Maddio, S., "A compact two-level sequentially rotated circularly polarized antenna array for C-band applications," *Int. J. of Antennas Propag.*, Vol. 2015, Art. ID 830920, Oct. 2015.
14. Castro, A. T. and S. K. Sharma, "Inkjet printed wideband circularly polarized microstrip patch array antenna on a PET film flexible substrate material," *IEEE Antennas Wireless Propag. Lett.*, Vol. 17, No. 1, 176–179, 2018.
15. Ta, S. X. and I. Park, "Low-profile broadband circularly polarized patch antenna using metasurface," *IEEE Trans. Antennas Propag.*, Vol. 63, No. 12, 5929–5934, Dec. 2015.
16. Luo, Q., F. Zhu, and S. Gao, *Circularly Polarized Antennas*, 6, Wiley (UK)-IEEE Press (USA), Jan. 2014.
17. Evans, H., P. Gale, B. Aljibouri, E. Lim, E. Korolkeiwicz, and A. Sambell, "Application of simulated annealing to design of serial feed sequentially rotated 2×2 antenna array," *Electron. Lett.*, Vol. 36, No. 24, 1987–1988, Nov. 2000.